Mechanization of a Robust Navigation Scheme for Land Applications Employing GNSS/INS Augmented with Zero Velocity Update

Muhammad Ushaq*, Merium F. Abbasi, and Muhammad R. U. B. Mirza

Department of Electronics Engineering, Center of Excellence for Science & Technology (CESAT), Islamabad, Pakistan
Email: ushaq71@yahoo.com (M.U.); abbasimerium@gmail.com (M.F.A.); rasheeq1@gmail.com (M.R.U.B.M)
*Corresponding author

Manuscript received February 20, 2024; revised March 25, 2024; accepted April 25, 2024; published September 25, 2024

***Abstract*—GNSS/INS Integrated Navigation systems mechanized for Land based applications face certain challenges especially near skyscraper, mountainous regions and high foliage environments wherein GNSS signals get interrupted. While Inertial Navigation System (INS) and Global Navigation Satellite System (GNSS) are widely used in augmentation but the integrated navigation solution can get compromised in GNSS-denied environments. This research work explores the integration of GNSS with low-cost Micro-Electromechanical System (MEMS) Inertial Measurement Unit (IMU) and Zero Update Position and Timing (ZUPT) rendering a robust navigation solution for land applications. ZUPT is used to mitigate accelerometers and gyroscope biases and resultantly it alleviates the errors in position, velocity and attitude especially in a GNSS-denied scenario. ZUPT is enabled when the host vehicle stops and velocity of the host vehicle becomes zero. ZUPT corrections employing Kalman Filter algorithms significantly contains the accumulated errors in position, velocity and attitude. The study investigates the impact of different types of errors (random, fixed and growing errors) in GNSS including complete unviability on the INS/GNSS integrated solution. It has been observed that, when time growing errors are introduced in GNSS output, it has the worst effect on its overall accuracy. To counteract potential degradation in position computation ensuing from GNSS denial or interruption, this work corroborates the efficacy of ZUPT. ZUPT updates strengthen the system's robustness and accuracy of INS/GNSS Integrated solution. The proposed scheme can be employed for any land application including autonomous commercial land vehicles, navigation in tunnels, mining work and pedestrian navigation system etc.**

***Keywords*—Inertial Navigation System (INS), Global Navigation Satellite System (GNSS), Kalman Filter, integrated navigation, GNSS errors, zero velocity correction, zero velocity update**

I. Introduction

In the past few decades the commercialization of autonomous land vehicles has brought a profound interest in design of robust navigation systems. Inertial Navigation System (INS) and Global Navigation Satellite System (GNSS) are the most eminent systems in the field of navigation in all mediums including land, air, space and submarine applications [1–3]. INS offer a distinctive advantage as a self-contained system, providing all-inclusive navigation solutions encompassing position, velocity, acceleration, attitude and attitude rates. However, relying on dead reckoning computations, INS is prone to unbounded error growth over time, due to the inherent biases in the sensors.

In contrast, GNSS maintain its accuracy within a bound mitigating the issue of error growth associated with INS. Therefore, when INS and GNSS are synergistically integrated, an optimal navigation solution is obtained, especially when uninterrupted availability of GNSS signals is ensured [4]. However, real world challenges such as signal jamming, spoofing, and obstruction of clear view of sky pose challenge to GNSS reliability [5]. This is particularly troublesome for land vehicle navigation applications in environments including tunnels, skyscrapers, mountains and dense forests. Resultantly, for longer duration applications, there is high probability of encountering the segments, where the availability of GNSS is compromised.

The zero velocity correction techniques can significantly improve the overall accuracy of land vehicle navigation. This is achieved by stopping the vehicle at certain periodic instances or at instances of user discretion. As the velocity becomes zero, this known information is fed as a correction to the INS and INS/GNSS Integrated solution for computing and correcting GNSS and INS errors. While the vehicle is stationary during stoppage, vehicle attitude (pitch, yaw and roll) can also be corrected. This scheme significantly renders improved position, velocity and attitude solution.

In this paper, effects of zero velocity correction are investigated by simulating different scenarios. To substantiate the presented scheme, first standalone Micro-Electromechanical System (MEMS) Inertial Measurement Unit (IMU) solution is presented. Subsequently, INS is integrated with GNSS when uninterrupted GNSS signals are available. Next, the segments of GNSS unavailability are introduced and their effect is studied. Furthermore, zero velocity update is incorporated. First, just INS is corrected by zero velocity and then it is used to improve the performance of INS and interrupted GNSS integrated navigation.

II. Related Work

Navigation in GNSS denied environments is a common problem being investigated and studied extensively by the navigators the world-over. A wide variety of solutions have been adopted to address this problem, ranging from incorporation of different aiding sensors to the use of machine learning algorithms for containing INS error during GNSS outages.

To ensure the robustness of land-based navigation using MEMS IMU and low cost GNSS receiver in urban environments with access to insufficient number of satellites, tightly coupled integration of INS and Precise Point Positioning (PPP) GNSS is performed using extended

Kalman filter [6]. This technique improves the robustness of navigation solution at the cost of additional computational load.

Mu *et al.* [7] presented the application of vehicle mode recognition algorithm and non-holonomic constraints to maintain the accuracy of MEMS-INS/GNSS integrated navigation for land vehicles in urban settings with GNSS outages. The application of this technique is limited by the estimating the accuracy of heading misalignment.

Another approach to maintain the accuracy of low-cost INS/GNSS solution in GNSS denied environment for land vehicles is presented by Chen *et al.* [8]. The position drift during the GNSS outages is controlled by using the stochastic model of time-differenced GNSS carrier phase, non-holonomic constraints and odometer measurements. However, this algorithm is not robust to frequent GNSS outages.

Chiang *et al.* [9] developed a navigation system for land vehicle using smartphone sensors for GNSS challenging environments. The data of IMU, GNSS and cameras is integrated using Extended Kalman Filter (EKF). The output of camera is processed by ORB-SLAM algorithm to compute velocity which is fed to the navigation algorithm.

Yang *et al.* [10] proposed a fault tolerant MEMS-INS/GNSS integrated navigation solution that is reliable under disturbances as well as partial and complete loss of GNSS data. It incorporates non-holonomic constraints and Allan-variance informed Kalman Filter.

Furthermore, Support Vector Machine (SVM) algorithm is employed by Cong *et al.* [11] to predict accumulation of MEMS-INS error during the intervals of GNSS outages. Dai *et al.* [12] demonstrated the application of recurrent neural networks (RNN) for INS/GNSS positioning in the absence of GNSS signals. Ushaq *et al.* [13] investigated and mitigated the effect of slowly growing errors in Global Positioning System (GPS) solutions, through adaptive Kalman Filtering algorithm. Another approach for successful positioning, despite satellite faults and data contamination is proposed by Li *et al.* [14]. To identify and exclude faulty GNSS measurements, graph optimization is used employing tightly coupled integration of INS and GNSS.

Most of the techniques employ either additional navigation aiding hardware or complex algorithm to maintain the accuracy of INS/GNSS positioning during GNSS outages. The additional sensors such as cameras, odometers and radars come with their own limitations, error sources and cost addition. The complexity of algorithms also directly translates into computational cost.

Zero velocity correction offers unique advantages without requiring additional hardware sensors or any significant increase in computational burden [15]. Although it has been employed along with other aids in various schemes presented in literature, but there was a lack of in-depth study on zero velocity correction and its direct impact on positioning accuracy during loss or contamination of GNSS signals which can be manifested in various forms. This study addresses this gap.

III. Inertial Navigation Systems (INS)

INS is based upon the input from three gyroscope and three accelerometers. Gyroscopes measure angular rates, whereas accelerometers measure translational acceleration. Inertial Navigation algorithm is used to compute position, velocity and attitude from accelerometers and gyroscope output, as shown in Fig. 1. In INS algorithm, the effect of gravity, earth's rotation and Coriolis force are compensated from accelerometer and gyroscope output, to compute instantaneous kinematic acceleration in navigation frame.

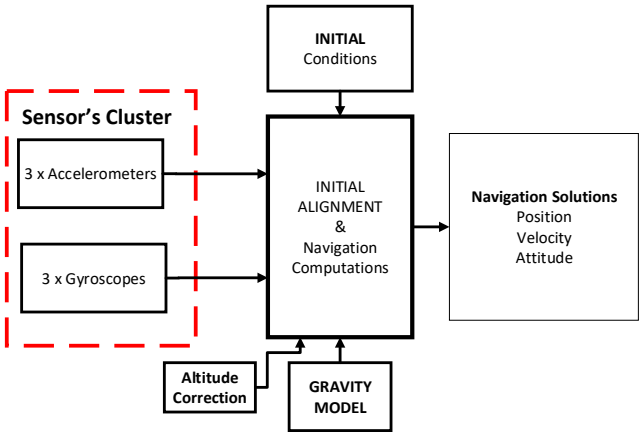

Fig. 1. Inertial navigation system.

In this paper, these computations are performed in local level north pointing East-North-Up (ENU) frame using the Eqs. (1)–(11).

Velocity computations:

$$\begin{bmatrix} \dot{V}_{ex}^{g} \\ \dot{V}_{ey}^{g} \\ \dot{V}_{ez}^{g} \end{bmatrix} = \begin{bmatrix} f_x^g \\ f_y^g \\ f_z^g \end{bmatrix} + \begin{bmatrix} 0 \\ 0 \\ g \end{bmatrix} - \begin{bmatrix} 0 & (2\omega_{iez}^{g} + \omega_{egz}^{g}) & -(2\omega_{iey}^{g} + \omega_{egy}^{g}) \\ -(2\omega_{iez}^{g} + \omega_{egz}^{g}) & 0 & (2\omega_{iex}^{g} + \omega_{egx}^{g}) \\ (2\omega_{iey}^{g} + \omega_{egy}^{g}) & -(2\omega_{iex}^{g} + \omega_{egx}^{g}) & 0 \end{bmatrix} \begin{bmatrix} V_{ex}^{g} \\ V_{ey}^{g} \\ V_{ez}^{g} \end{bmatrix} \quad (1)$$

whereas, $\begin{bmatrix} f_x^g & f_y^g & f_z^g \end{bmatrix}^T$ are the outputs of accelerometers transformed in ENU Frame.

$$V_e^g(t_{n+1}) = V_e^g(t_n) + \int_{t_n}^{t_{n+1}} \dot{V}_e^g dt \quad (2)$$

Position (Latitude, Longitude and Altitude) Computations:

$$\dot{\phi} = \frac{V_y^g}{R_M + h} \quad (3)$$

$$\dot{\lambda} = \frac{V_x^g}{(R_N + h)Cos\phi} \quad (4)$$

$$h(t_{n+1}) = h(t_n) + \int_{t_n}^{t_{n+1}} V_{ez}^g dt \quad (5)$$

whereas:

$$R_M = R_e\left(1 - 2e + 3eSin^2\phi\right) \quad (6)$$

$$R_N = \mathrm{R}_e\left(1 + eSin^2\phi\right) \quad (7)$$

Are meridian and transverse radii of curvatures of the Earth.

Direction Cosine Matrix from Navigation Frame to Body Frame is computed as follows:

$$C_g^b = \begin{bmatrix} Cos\gamma Cos\psi + Sin\gamma Sin\theta Sin\psi & -Cos\gamma Sin\psi + Sin\gamma Sin\theta Cos\psi & -Sin\gamma Cos\theta \\ Cos\theta Sin\psi & Cos\theta Cos\psi & Sin\theta \\ Cos\gamma Cos\psi - Cos(\gamma) Sin\theta Sin\psi & -Sin\gamma Sin\psi - Cos\gamma Sin\theta Cos\psi & Cos\gamma Cos\theta \end{bmatrix} \quad (8)$$

Attitude (yaw, pitch, roll) Computations:

$$\psi_g = tan^{-1}(\frac{C_{g21}^b}{C_{g22}^b}) \quad (9)$$

$$\theta_g = Sin^{-1}(C_{g23}^b) \quad (10)$$

$$\gamma_g = tan^{-1}(-\frac{C_{g13}^b}{C_{g33}^b}) \quad (11)$$

Detail of all variables mentioned in above equations can be found in [3].

The instantaneous acceleration can be integrated to compute velocity, which can be integrated again for position calculation. Due to this integration, the slight errors in sensors and non-kinematic compensations accumulate significantly resulting in unbounded growth in final position and velocity errors.

IV. Global Navigation Satellite System (GNSS)

GNSS is considered as the most popular and reliable navigation systems, presently. It relies on number of satellites orbiting around the Earth along know orbits with known Orbital (Keppler) parameters all the time. These satellites transmit signals traveling with the speed of light, containing the information including satellite position, transmission time and other parameters. The receivers at user location can compute their position by using the difference in transmission and arrival time employing TRILATERATION scheme. However, if errors are introduced anywhere during this process, they can degrade the accuracy of computed position [16].

A. Clock Errors

Satellite clocks are generally very accurate. If any deviation appears in them, monitoring stations estimate correction parameters and send them to the receivers. However, the receiver clocks are inexpensive to ensure affordability. Therefore, they have inherent biases, which if not compensated accurately, introduce error is the position estimation.

B. Ionospheric and Tropospheric/Stratospheric Delays

The GNSS signals travel through the ionosphere. The ionization can affect the transit time of the signal. Since the ionization level keep on changing with the solar activity, the transit time error cannot be predicted precisely unless dual frequency receivers are used. Furthermore, variability in satellite elevation also affect the ionospheric delays. After ionosphere, signals have to cross the troposphere. Although troposphere is electron neutral, it introduces dry and wet components of errors as it slows down the signal because of it being refractive.

C. Multipath Error

Multipath error: It is a source of major concern in urban settings. Due to the tall buildings and other obstructions the GNSS signal is reflected. It reaches the receiver indirectly with a delay and higher signal to noise ratio. Apart from that, error is also introduced due to inherent noise in receiver caused by thermal noise, circuitry, signal sampling and quantization.

Other types of GNSS errors include those due to jamming, spoofing and thermal variation in GNSS receivers.

These errors manifest themselves in different forms in final position and velocity of GNSS. Sometimes the result in increased randomness in final solution, at other times fixed or growing errors are introduced. There are also cases when there is no output at all.

V. Zero Update Position and Timing (ZUPT)

ZUPT also known as zero velocity update is performed by stopping the vehicle or any other host system and getting information about zero velocity with certainty. This information can reduce the overall uncertainty in positioning which generally keeps on growing with time due to respective errors of INS and GNSS.

In manual ZUPT application ZUPT is initiated at driver/user discretion after manual stopping of the vehicle. In automatic ZUPT applications, there are various ways to detect periodic zero velocity. Some are based on hardware and other are software based. In hardware-based methods, usually the output of odometer is used to infer the occurrences of zero velocity. The software-based techniques include adaptive thresholding, cycle segmentation, and other data driven classifiers [10].

VI. INS/GNSS/ZUPT Integration

Kalman Filter algorithm is used for GNSS/INS/ZUPT Integration. It is a two-step predictor-corrector estimator. The first step involves prediction of the state and the second corrects it using the measurement. The predictor equations are:

$$\hat{x}_{k/k-1} = \Phi_{k,k-1}\hat{x}_{k-1} \quad (12)$$

$$P_{k/k-1} = \Phi_{k,k-1}P_{k-1}\Phi_{k,k-1}^T + \Gamma_{k-1}Q_{k-1}\Gamma_{k-1}^T \quad (13)$$

The corrector equations are:

$$K_k = P_{k/k-1}H_k^T(H_kP_{k/k-1}H_k^T + R_k)^{-1} \quad (14)$$

$$\hat{x}_k = \hat{x}_{k/k-1} + K_k(z_k - H_k\hat{x}_{k/k-1}) \quad (15)$$

$$P_k = (I - K_kH_k)P_{k/k-1}(I - K_kH_k)^T + K_kR_kK_k^T \quad (16)$$

where

$\Phi_k \in \Re^{n\times n}$ is a system state transition matrix at epoch *k*.

$x_k \in \Re^n$ is a state vector

Γ_k is the KF model noise matrix it relates the system noise vector w_k to the system state vector x_k

$w_k \in \Re^n$ represents the system noise characterized by the matrix Q (Covariance of System noise)

$z_k \in \Re^p$ is the measurement vector

$H_k \in \Re^{p\times n}$ is the measurement matrix and relates the state vector x_k to the measurement z_k vector.

$v_k \in \Re^{p}$ is the measurement noise. The precision of sensors is indicated by a covariance matrix R

Kalman filter is based on the assumption that the state vector $\hat{x}$, estimation error vector $\tilde{x} = x - \hat{x}$, system noise vector (w) and measurement errors vector (v) are all Gaussian in nature, uncorrelated and expressed by following statistical expressions:

$$E\left[\tilde{x}_k \tilde{x}_j^{\,T}\right] = P_k \text{ for k=j, 0 for } k \neq j$$

$$E\left[w_k v_j^{\,T}\right] = 0 \text{ for all values of k and j}$$

$$E\left[w_k w_j^{\,T}\right] = Q_k \text{ for k=j, 0 for } k \neq j$$

$$E\left[v_k v_j^{\,T}\right] = R_k \text{ for k=j, 0 for } k \neq j$$

It may be noted that $Q \in \Re^{p\times p}$ and $R_k \in \Re^{m\times m}$ are positive definite matrices. p and m are the sizes of system noise vector(w) and measurement noise vector(v) respectively. Where $E[\cdot]$ denotes the expectation, and δ_{ij} is the Kronecker delta function. Initial state x_0 is normally distributed with zero mean and covariance P_0.

In this paper, INS error equations are used in prediction mode. The correction is performed by using GNSS or zero-velocity measurement. Here, x_k is error state vector with dimensions of 15×1.

$$x = \left[\varphi_x \quad \varphi_y \quad \varphi_z \quad \delta V_x^g \quad \delta V_y^g \quad \delta V_z^g \quad \delta\phi \quad \delta\lambda \quad \delta h \ldots \quad \varepsilon_{bx} \quad \varepsilon_{by} \quad \varepsilon_{bz} \quad \nabla_{bx} \quad \nabla_{by} \quad \nabla_{bz}\right]^T \tag{17}$$

Components of x_k in Eq. (17) are errors in pitch, roll, yaw, east velocity, north velocity, up velocity, latitude, longitude, altitude, three gyro errors and three accelerometer errors, respectively.

P is the error covariance matrix, which represent the estimated stability of the state vector. Its diagonal elements are variances of error of individual elements of the state vector.

$$P = diag\begin{pmatrix} \sigma_{\varphi_E}^2 & \sigma_{\varphi_N}^2 & \sigma_{\varphi_U}^2 & \sigma_{\delta V_E}^2 & \sigma_{\delta V_N}^2 & \sigma_{\delta V_U}^2 & \sigma_{\delta\phi}^2 & \sigma_{\delta\lambda}^2 \ldots \\ \sigma_{\delta h}^2 & \sigma_{\varepsilon_{bx}}^2 & \sigma_{\varepsilon_{by}}^2 & \sigma_{\varepsilon_{bz}}^2 & \sigma_{\nabla_{bx}}^2 & \sigma_{\nabla_{by}}^2 & \sigma_{\nabla_{bz}}^2 & \end{pmatrix} \tag{18}$$

Q is a process noise covariance matrix, representing uncertainty in the process model. In this case, it comprises of covariance of accelerometers and gyroscopes errors.

$$Q = diag\left[\sigma_{gx}^2 \quad \sigma_{gy}^2 \quad \sigma_{gz}^2 \quad \sigma_{ax}^2 \quad \sigma_{ay}^2 \quad \sigma_{az}^2\right] \tag{19}$$

For INS/GNSS integration, the measurement vector is given by:

$$z = \begin{bmatrix} \hat{V}_{ix}^g \\ \hat{V}_{iy}^g \\ \hat{V}_{iz}^g \\ \hat{\phi}_i(Rm+h) \\ \hat{\lambda}_i(R+h)Cos\phi_i \\ \hat{h}_i \end{bmatrix} - \begin{bmatrix} \hat{V}_{Gx}^g \\ \hat{V}_{Gy}^g \\ \hat{V}_{Gz}^g \\ \hat{\phi}_G(Rm+h) \\ \hat{\lambda}_G(R+h)Cos\phi_G \\ \hat{h}_G \end{bmatrix} \tag{20}$$

The measurement matrix which maps the measurement vector to state vector is given by *H*:

$$H = \begin{bmatrix} 0&0&0&1&0&0&0&0&0&0&0&0&0&0&0 \\ 0&0&0&0&1&0&0&0&0&0&0&0&0&0&0 \\ 0&0&0&0&0&1&0&0&0&0&0&0&0&0&0 \\ 0&0&0&0&0&0&(R_M+h)&0&0&0&0&0&0&0&0 \\ 0&0&0&0&0&0&0&(R_N+h)\cos\phi&0&0&0&0&0&0&0 \\ 0&0&0&0&0&0&0&0&1&0&0&0&0&0&0 \end{bmatrix} \tag{21}$$

The measurement noise covariance matrix, R, represent uncertainty in measurement. In this case, it is the error of GNSS output. It is given by:

$$R = diag\left[\sigma_{V_{Gx}}^2 \quad \sigma_{V_{Gy}}^2 \quad \sigma_{V_{Gz}}^2 \quad \sigma_{\phi_G}^2 \quad \sigma_{\lambda_G}^2 \quad \sigma_{h_G}^2\right] \tag{22}$$

When zero velocity is detected, the measurement vector is:

$$z = \begin{bmatrix} \hat{V}_{ix}^g \\ \hat{V}_{iy}^g \\ \hat{V}_{iz}^g \end{bmatrix} - \begin{bmatrix} \hat{V}_{Gx}^g \\ \hat{V}_{Gy}^g \\ \hat{V}_{Gz}^g \end{bmatrix} \tag{23}$$

And measurement covariance matrix is:

$$R = diag\left[\sigma_{V_{Gx}}^2 \quad \sigma_{V_{Gy}}^2 \quad \sigma_{V_{Gz}}^2\right] \tag{24}$$

Measurement Matrix

$$\boldsymbol{H} = \left[zeros\ 3,3) \quad eye(3,3) \quad zeros(3,9)\right] \tag{25}$$

VII. Simulations and Results

The simulations for land vehicle navigation were performed in 2D for the period of about one hour. Initially the vehicle is stationary for 1 min. After accelerating, it traverses a 2D trajectory with the speed of around 10 m/s. After travelling for around 40 min, the vehicle comes to rest again.

The MEMS IMU with accelerometers of 0.2 mg random bias and gyroscopes of 5º/hr random bias were used. The GNSS receiver with the of 25 m random errors in position and 0.1 m/s random velocity error was incorporated.

A. Standalone INS

When only MEMS IMU is used for navigation, considerable error was introduced. The navigation solution does not follow the trajectory well as shown in Fig. 2. Although, the motion is in 2D, the vertical velocity is introduced as indicated by Fig. 3. Fig. 4 shows the introduction of maximum of 2 km of error in latitude and longitude during 45 min. Fig. 5 indicates the position error of INS stand-alone system.

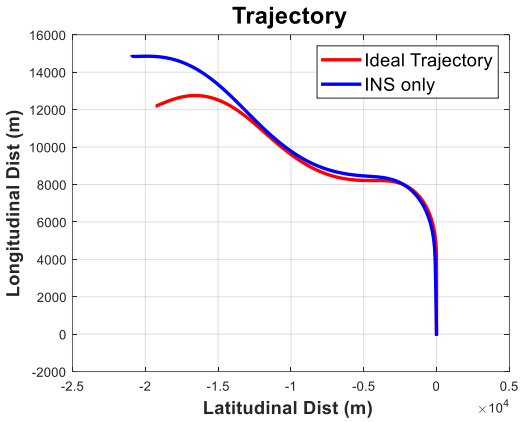

Fig. 2. Standalone INS trajectory.

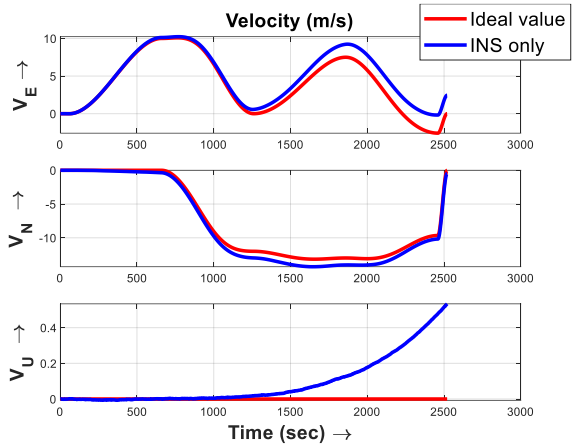

Fig. 3. Standalone INS velocity.

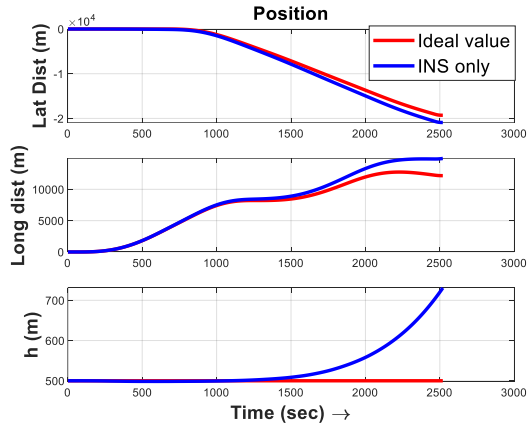

Fig. 4. Standalone INS position.

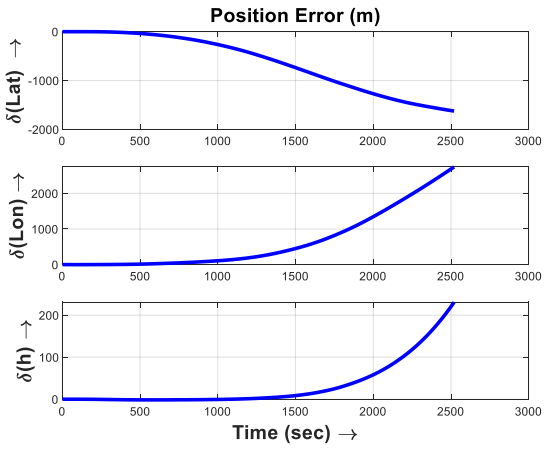

Fig. 5. Position error of standalone INS.

B. *INS/GNSS Integration*

When INS and GNSS are integrated, the final navigation solution is almost coincident to ideal values as shown in Fig. 6. East, North and Up velocities are plotted in Fig. 7. Position computed by INS/GNSS Integration is plotted vis a vis reference values in Fig. 8. The position errors converge to zero as depicted by Fig. 9. This is the case only if GNSS is available without any interruptions.

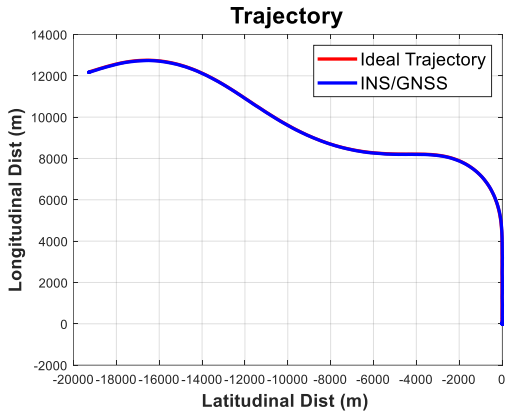

Fig. 6. INS/GNSS integrated trajectory.

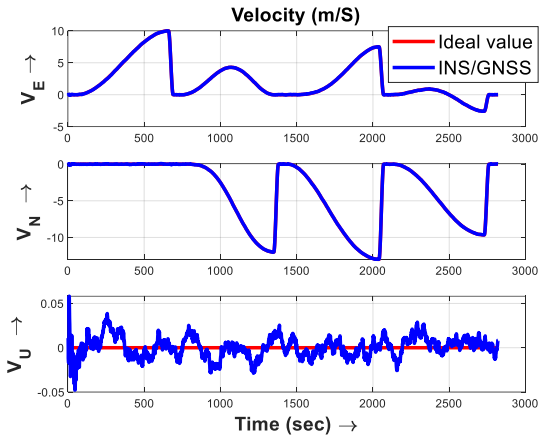

Fig. 7. INS/GNSS integrated velocity.

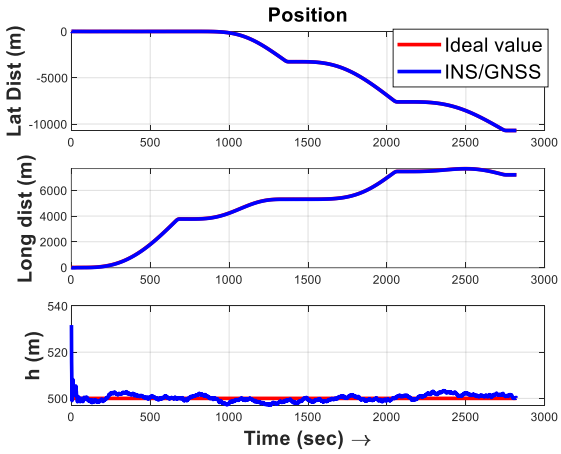

Fig. 8. INS/GNSS integrated position.

C. *INS with Interrupted GNSS*

Due to the multitude of factors, an un-interrupted availability of GNSS is not possible in normal urban settings. As a result, different types of disturbances are introduced.

In this case, there was interruption in GNSS from 18–25 min and then from 32–35 min.

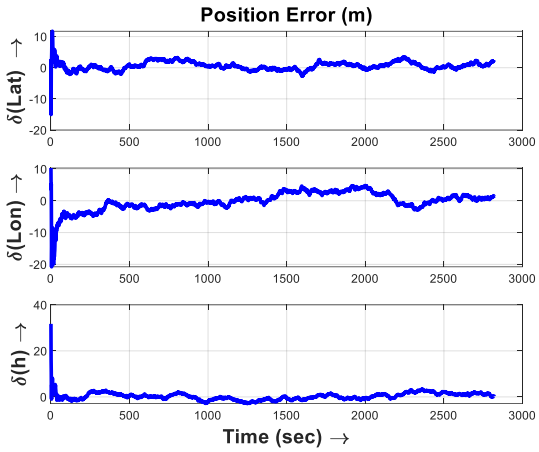

Fig. 9. Position error of INS/GNSS integration.

Case 1: In the first case, as a result of interruption, a random noise is introduced in the output of GNSS. Here, in the interrupted segment, the randomness in GNSS output was increased to 10 times.

The effect of the randomness in GNSS is reflected in the final navigation solution. The INS/GNSS trajectory exhibit some deviation from the ideal one as shown in Fig. 10. The velocity and position error clearly show the effect of randomness Fig. 11.

Case 2: Instead of random errors, if growing errors are introduced in GNSS, they can create havoc as shown in Fig. 12. Although Kalman filter tries to arrest the errors back as soon as GNSS become available again, but still the overall error significantly degrades the solution. Fig. 13 shows the velocity solutions in case of interrupted GNSS signals.

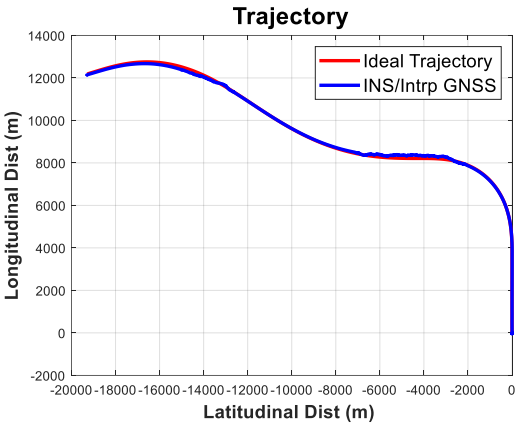

Fig. 10. Trajectory of INS/GNSS Integ having random errors.

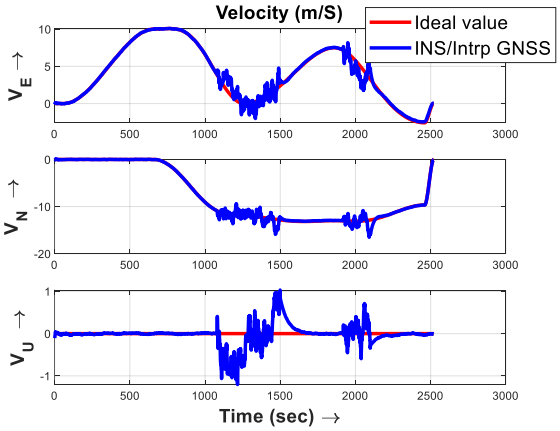

Fig. 11. Velocity of INS/GNSS Integ having random errors.

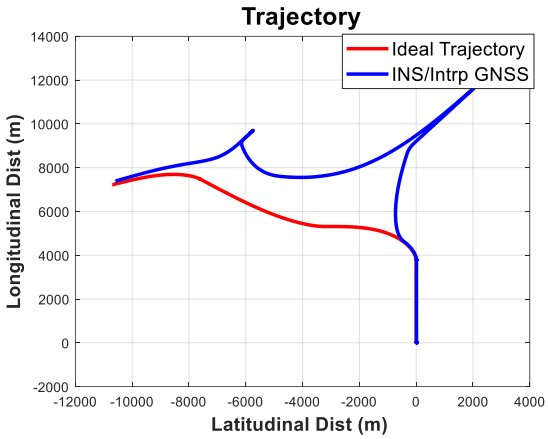

Fig. 12. Trajectory of INS/GNSS Integ having growing errors.

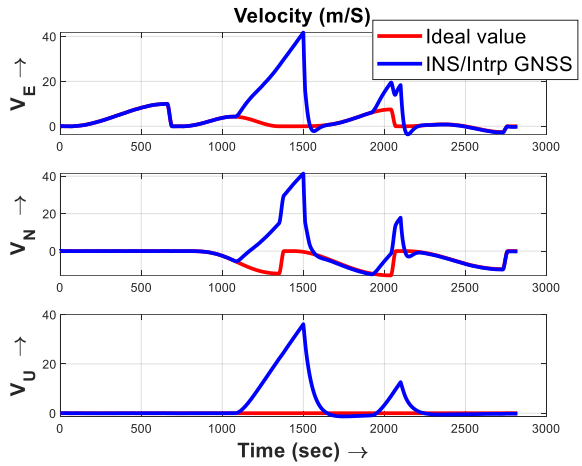

Fig. 13. Velocity of INS/GNSS Integ with growing errors.

D. *INS/ZUPT Integration*

If standalone INS is aided by zero-velocity correction, it can somewhat reduce the final navigation errors. Here, the two important factors are the accuracy of INS sensors and frequency of zero-velocity. Increasing either of them, improves the final solution. However, the price of high accuracy INS becomes prohibitively high for most of applications. Increasing the frequency of zero-velocity correction is also not very feasible as it requires stopping the vehicle for some finite time.

In this case, zero-velocity correction was performed after every 10 min. As vehicle was already stationary initially, it was stopped for first velocity correction after 10 min (around 1200 secs). After 10 min, the vehicle was decelerated, then stopped for 1 min and then accelerated again. As it was stopped thrice, the overall time has increased for the same total distance. Every time, the vehicle is stopped, the error in velocity becomes zero. However, during the next 10 min interval, when it is operating under pure INS, the error grows again.

The final trajectory of INS and zero velocity corrected solution does not coincide with the ideal trajectory, but still it is improved version of standalone Fig. 14 INS. If the frequency of zero velocity update or sensor accuracy is enhanced, even better results can be obtained.

As the time passes, the growth becomes more significant as shown in Figs. 15 and 16.

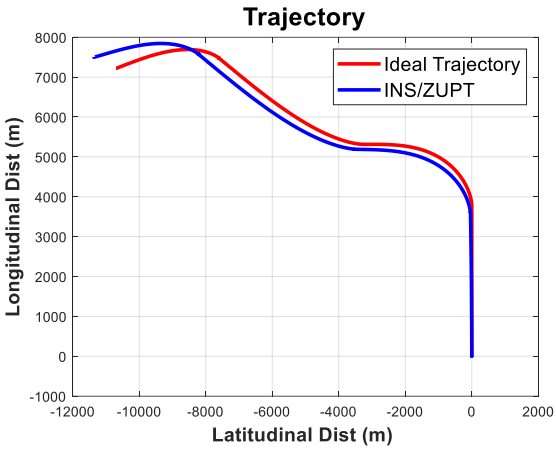

Fig. 14. INS/ZUPT trajectory.

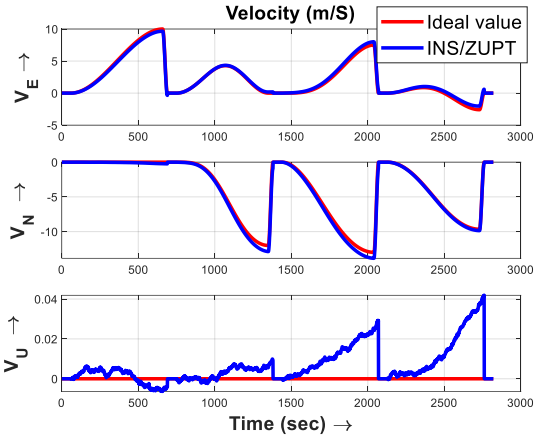

Fig. 15. INS/ZUPT velocity.

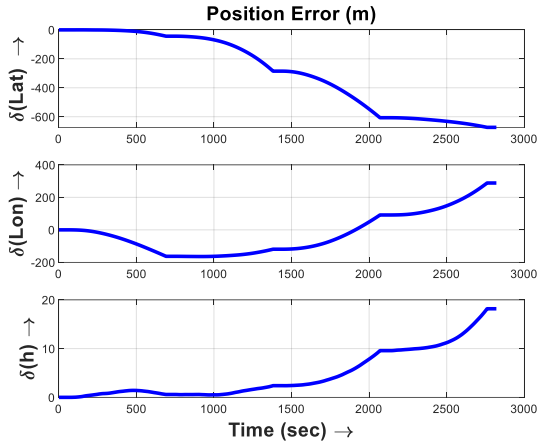

Fig. 16. INS/ZUPT position error.

E. *INS/Interrupted GNSS/ZUPT Integration*

When INS, GNSS with interruptions, and zero-velocity correction are integrated, the final navigation solution is significantly improved Fig. 17.

When GNSS becomes unavailable, the error is introduced. However, if the zero-velocity correction of 1 min after every 10 min is performed, the final errors stays within bounds even if the GNSS interruption result in the growing errors (Figs. 18 and 19).

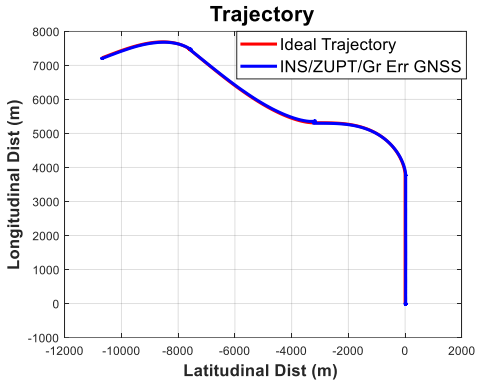

Fig. 17. INS/Interrupted GNSS/ZUPT trajectory.

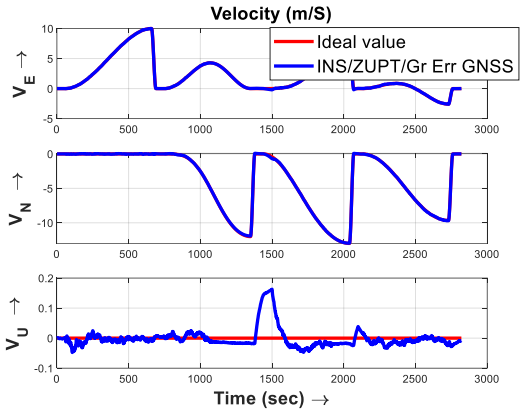

Fig. 18. INS/Interrupted GNSS/ZUPT velocity.

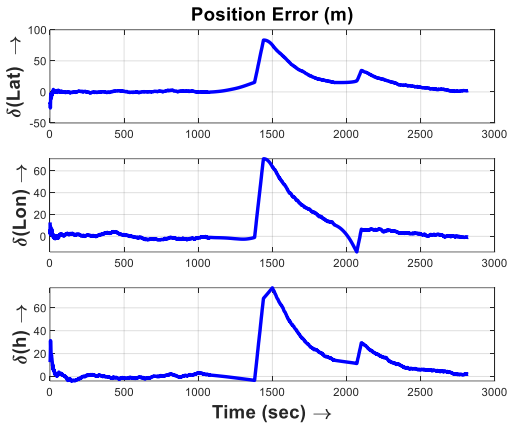

Fig. 19. INS/Interrupted GNSS/ZUPT position error.

VIII. Conclusion

The standalone INS give the complete and self-contained navigation solution. But due to error accumulation, the INS solution after few minutes becomes overly erroneous for many practical applications, unless highly precise and expensive sensors are used. Therefore, in most scenarios, standalone INS is not employed. The integration of INS with GNSS is the most common practice since the two systems have complementary properties. Nevertheless, there are some sources of errors in GNSS as well which can manifest themselves in different forms. They can introduce growing errors in GNSS position and velocity, increase randomness by several orders of magnitude or can result in null output. In this paper, the two cases of manifestation of GNSS errors are

studied. In case of increased randomness, the integrated trajectory might not deviate significantly. But when there is a growing error in GNSS, it completely deteriorates the navigation solution. If zero velocity update is incorporated by stopping the vehicle after some periodic intervals for a short time, the final solution can be significantly improved both in the case of growing and random errors of GNSS.

Conflict of Interest

The authors declare no conflict of interest.

Author Contributions

Dr. Muhammad Ushaq developed the algorithms. Merium Fazal Abbasi analyzed the data. Dr. Muhammad Rasheeq Ullah Baig Mirza contributed in the experiments. All authors had approved the final version.

References

[1] D. Titterton and L. John, *Strapdown Inertial Navigation Technology*, 2nd ed. 2004.

[2] J. Farrell, *Aided Navigation: GPS with High Rate Sensors*, McGraw Hill LLC, 2008.

[3] M. Ushaq and C. Y. Zhang, "Research on SINS based navigation techniques," M.S. thesis, Beihang University, Beijing, 2004.

[4] P. D. Groves, *Principles of GNSS, Inertial, and Multisensor Integrated Navigation Systems*, Artech House, 2008.

[5] M. Ushaq and J. Fang, "Enhanced performance information fusion techniques for integrated navigation systems realized through modern fault tolerant filtering methodologies," M.S. thesis, Beihang University, Beijing, 2013.

[6] Y. Liu, F. Liu, Y. Gao, and L. Zhao, "Implementation and analysis of tightly coupled Global Navigation Satellite System Precise Point Positioning/Inertial Navigation System (GNSS PPP/INS) with insufficient satellites for land vehicle navigation," *Sensors*, vol. 18, no. 12, Dec. 2018.

[7] M. Mu and L. Zhao, "A GNSS/INS-integrated system for an arbitrarily mounted land vehicle navigation device," *Gaps Solution*, no. 112, Apr. 2019.

[8] C. Chen and G. Chang, "Low-cost GNSS/INS integration for enhanced land vehicle performance," *Meas. Sci. Technol.*, 03009, Mar. 2019.

[9] K.-W. Chiang, T. T. Duong, and J.-K. Liao, "The performance analysis of a real-time integrated INS/GPS vehicle navigation system with abnormal GPS measurement elimination," *Sensors*, pp. 10599–10622, Aug. 2013.

[10] L. Yang, Y. Li, Y. Wu, and C. Rizos, "An enhanced MEMS-INS-GNSS integrated system," *GPS Solutions*, vol. 18, pp. 593–603, 2014.

[11] L. Cong, S. Yue, H. Qin, B. Li, and J. Yao, "Implementation of a MEMS-based GNSS/INS integrated scheme using supported vector machine for land vehicle navigation," *IEEE Sensors*, vol. 20, no. 23, pp. 14423–14435, 2020.

[12] H. F. Dai, H. W. Bian, R. Y. Wang, and H. Ma, "An INS/GNSS integrated navigation in GNSS denied environment using recurrent neural network," *Elsevier*, vol. 16, no. 2, pp. 334–340, 2020.

[13] M. Ushaq, J. Fang, and J. Ali, "An adaptive & fault tolerant sins/GPS integrated navigation scheme robustified against slowly growing errors in GPS updates.," *Applied Mechanics and Materials*, vol. 390, pp. 500–505, 2013.

[14] W. Li, X. Cui, and M. Lu, "A robust graph optimization realization of tightly coupled GNSS/INS integrated navigation system for urban vehicles," *Tsinghua Sci Technol*, pp. 724–732, Jun. 2018.

[15] J. Wahlström and Skog, "Fifteen years of progress at zero velocity: A review," *IEEE Sens. J.*, pp. 1139–1151, Feb. 2020.

[16] A. Noureldin, B. K. Tashfeen, and G. Jacques, *Fundamentals of Inertial Navigation, Satellite-Based Positioning and Their Integration*, Springer Science & Business Media, 2012.